Available online at www.sciencedirect.com
ScienceDirect
Mendeleev Communications
Mendeleev Commun., 2018, **28**, 418–420

New all-*cis*-tetra(*p*-tolyl)cyclotetrasiloxanetetraol and its functionalization

Yuliya S. Vysochinskaya,[a,b] Anton A. Anisimov,[a] Sergey A. Milenin,[b] Alexander A. Korlyukov,[a] Fedor M. Dolgushin,[a] Elena G. Kononova,[a] Alexander S. Peregudov,[a] Mikhail I. Buzin,[a] Olga I. Shchegolikhina*[a] and Aziz M. Muzafarov[a,b]

[a] *A. N. Nesmeyanov Institute of Organoelement Compounds, Russian Academy of Sciences, 119991 Moscow, Russian Federation. E-mail: olga@ineos.ac.ru*

[b] *N. S. Enikolopov Institute of Synthetic Polymeric Materials, Russian Academy of Sciences, 117393 Moscow, Russian Federation*

DOI: 10.1016/j.mencom.2018.07.026

New all-*cis*-tetra(*p*-tolyl)cyclotetrasiloxanetetraol and its derivatives with Si(CH=CH$_2$)Me and Si(H)Me$_2$ groups have been prepared and characterized by IR and NMR spectroscopy, GPC, mass spectrometry, TGA and DSC. Molecular and crystalline structures of the tetraol and its derivative with four Si(CH=CH$_2$)Me groups have been determined by single-crystal X-ray diffraction.

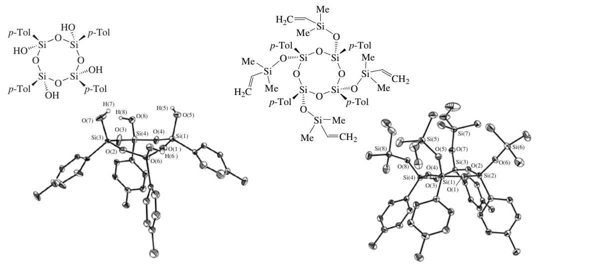

Preparation of polyorganosilsesquioxane polymers of various molecular masses and architecture exhibiting a complex of valuable physical and chemical properties is an actual task of the modern materials science.[1–9] Production of cyclosiloxane tetraols as initial monomeric units for target synthesis of polyorganosilsesquioxane polymers is an area of vigorous scientific activity.[10–18] However, the methods used for the various tetraol preparations[10–14,16] based on hydrolytic condensation of organotrichloro- and organotrialkoxysilanes have a number of disadvantages, for example, the use of HCl acceptors, multistaging and low selectivity. The method that we previously[15,17,19] developed implements the principle of metal ion-directed self-assembly pathway to selectively form individual organometallasiloxane molecules by means of hydrolytic condensation of various trifunctional organoalkoxysilanes in the presence of ions of alkali and transition metals. The subsequent reaction of the organometallasiloxanes with dilute hydrochloric acid or acetic acid in organic solvents allows the metal ions to be effectively removed thus giving siloxane cyclic polyols.[15,17] In our opinion, the synthesis of siloxane tetraols with modified phenyl group suitable for further chemical transformation and the study of their properties can be of special interest for the preparation of new type of amphiphilic star-shaped polysiloxanes with tailor-made properties.

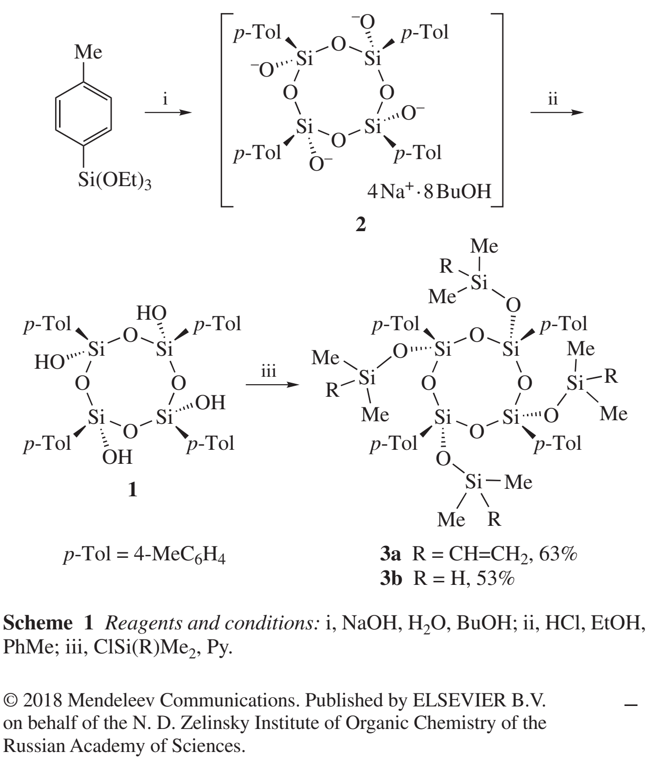

Scheme 1 *Reagents and conditions:* i, NaOH, H$_2$O, BuOH; ii, HCl, EtOH, PhMe; iii, ClSi(R)Me$_2$, Py.

Here, we present the synthesis of all-*cis*-1,3,5,7-tetra(*p*-tolyl)-1,3,5,7-tetrahydroxycyclotetrasiloxane **1** and the study of its structure and properties using the single-crystal and powder X-ray diffraction, DSC, IR and NMR spectroscopy. The synthesis of compound **1** was performed in two stages (Scheme 1). First, crystalline sodium *cis*-1,3,5,7-tetra(*p*-tolyl)-1,3,5,7-cyclotetrasiloxanolate **2** was prepared by the hydrolytic condensation of *p*-tolyltriethoxysilane in the presence of equimolar amount of sodium hydroxide and water in *n*-butanol[20] (see Scheme 1). The treatment of salt **2** with dilute hydrochloric acid in ethanol–toluene mixture affords white crystals of product **1** in 77% yield.

Based on compound **1**, we obtained the new functional stereoregular cyclotetrasilsesquioxanes **3a**,**b** by its reaction with the corresponding dimethylchlorosilanes (see Scheme 1). These compounds bear functional Me$_2$Si(CH=CH$_2$) (**3a**) or Me$_2$Si(H) (**3b**) groups at the Si atom on one side of the ring skeleton and a hidden functional *p*-tolyl group at the Si atoms on the opposite side.

Molecular structures of obtained compounds **1** and **3a** are shown in Figure 1.† Eight-membered tetrasiloxane cycle in the molecule of **1** is folded over the line between opposite silicon atoms (the bending angles are close to 30°). Eight-membered tetrasiloxane cycle in the molecule of **3a** has a more flattened conformation with six endocyclic atoms in plane (mean deviation is 0.06 Å) and the rest two atoms, namely Si(3) and O(2), deviate

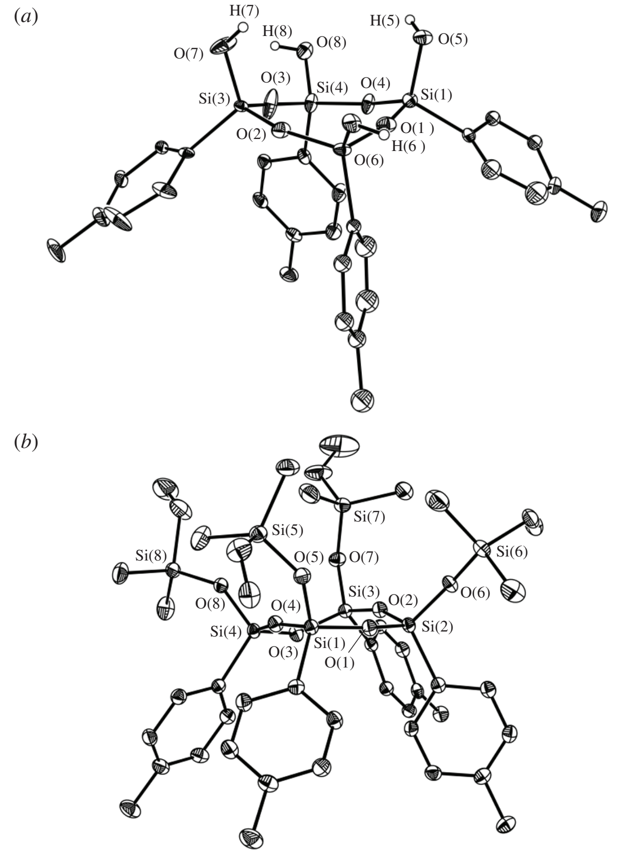

Figure 1 Molecular structures of compounds (*a*) **1** (one of two independent molecules is shown) and (*b*) **3a**. Thermal ellipsoids are drawn at the 30% probability level, hydrogen atoms excluding hydroxyl groups in **1** are omitted for clarity. Selected bond lengths (Å): Si–O (endocyclic) 1.593(3)–1.620(2) ⟨1.612⟩ (**1**), 1.603(3)–1.613(3) ⟨1.609⟩ (**3a**), Si–O (exocyclic) 1.601(3)–1.633(3) ⟨1.623⟩ (**1**), 1.591(3)–1.611(3) ⟨1.602⟩ (**3a**). Selected bond angles (°): Si–O–Si (endocyclic) 149.3(2)–164.5(2) ⟨155.9⟩ (**1**), 142.5(2)–163.5(2) ⟨154.2⟩ (**3a**).

from this plane by 0.62 and 0.57 Å, respectively. Consequently, four silicon atoms in eight-membered tetrasiloxane cycles adopt a butterfly arrangement in the molecule of **1** and almost square-planar arrangement in the molecule of **3a**.

All hydroxyl groups in the molecule of **1** are included in the H-bonded tubelike chain formation with the intermolecular O···O distances being from 2.667(4) to 2.786(4) Å. The analogues tube-like chains were detected only in co-crystal of all-*cis*-$[Pr^iSi(O)OH]_4$ with $Pr^i_2Si(OH)_2$,[23] however in case of **1** the chains are constructed with tetrasiloxanetetraol molecules only. In most published crystal structures of cyclic tetrasiloxanetetraols $[RSi(O)OH]_4$, the molecules were assembled by O–H···O bonds into layered (2D) supramolecular associates.[10–12,14,17,21,22]

† *Crystal data for* **1**. $C_{28}H_{32}O_8Si_4$ (M = 608.89), triclinic, space group $P\bar{1}$, a = 15.5244(3), b = 15.9252(3) and c = 15.9405(3) Å, α = 103.1449(11)°, β = 113.4462(12)°, γ = 101.8319(13)°, V = 3322.62(11) Å^3, Z = 4, d_{calc} = = 1.217 g cm^{-3}, μ(CuKα) = 20.29 cm^{-1}, θ_{max} = 71.7°. Total of 12426 unique reflections (R_{int} = 0.0642) were measured, from which 10181 [$I > 2\sigma(I)$] were used for refinement, 748 parameters, R_1 = 0.0677, wR_2 = = 0.1830, GOOF = 1.061.

Crystal data for **3a**. $C_{44}H_{64}O_8Si_8$ (M = 945.67), triclinic, space group $P\bar{1}$, a = 11.332(3), b = 11.930(3) and c = 20.029(5) Å, α = 80.694(4)°, β = 81.979(4)°, γ = 76.573(4)°, V = 2584.3(12) Å^3, Z = 2, d_{calc} = 1.215 g cm^{-3}, μ(MoKα) = 2.54 cm^{-1}, θ_{max} = 27.0°. Total of 11277 unique reflections (R_{int} = 0.0599) were measured, from which 7862 [$I > 2\sigma(I)$] were used for refinement, 553 parameters, R_1 = 0.0671, wR_2 = 0.1829, GOOF = 1.111.

CCDC 1589864 and 1589865 contain the supplementary crystallographic data for this paper. These data can be obtained free of charge from The Cambridge Crystallographic Data Centre *via* http://www.ccdc.cam.ac.uk.

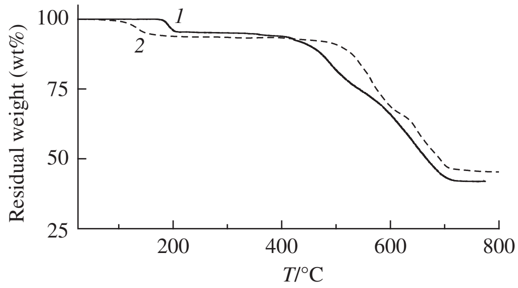

Figure 2 TGA curves for (*1*) **1** and (*2*) *cis*-$[PhSi(O)OH]_4$ at a heating rate 10 K min^{-1} in air.

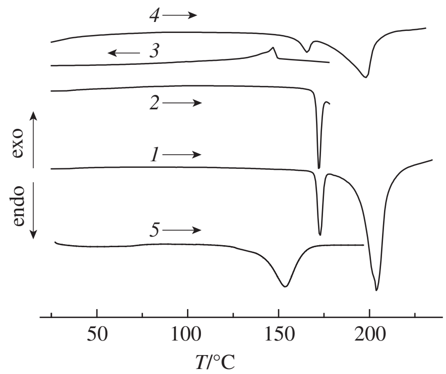

Figure 3 DSC traces for (*1–4*) **1** and (*5*) *cis*-$[PhSi(O)OH]_4$ upon (*1*), (*2*), (*5*) first, (*4*) second heating and (*3*) cooling. Heating rate was 10 K min^{-1} in air.

The TGA and DSC data obtained for product **1** are presented in Figures 2 and 3. To study the effect of Me substituent introduction in phenyl ring, we compared thermal behavior of compound **1** with that of *cis*-1,3,5,7-tetraphenyl-1,3,5,7-tetrahydroxy-cyclotetrasiloxane $[PhSi(O)(OH)]_4$ sample.

The TGA analysis of **1** (see Figure 2, curve *1*) reveals the presence of a mass loss stage (5 wt%) in the temperature range 165–212 °C. The DSC curve *1* obtained upon heating (see Figure 3) demonstrates two endothermic peaks in the same temperature range. The first one is sharp, with the maximum at 172 °C (ΔH = 18 J g^{-1}). The second peak is wide, with the maximum at 204 °C (ΔH = 100 J g^{-1}). Heating of the sample to 176 °C (the end of the first endotherm (see Figure 3, curve *2*), cooling to the room temperature (curve *3*) and the subsequent heating (curve *4*) have shown that the transition is reversible. However, upon the repeated heating of the sample, the temperature and heat prove to be perceptibly lower (165 °C and 12 J g^{-1}, respectively), the second endothermic peak also shifts to a lower temperature (198 °C) and is characterized by a substantially lower transition heat (ΔH = 56 J g^{-1}). The above results suggest that the reversible endotherm at 172 °C originates from the melting of crystalline phase of compound **1**. This process goes simultaneously with the thermal polycondensation of OH groups in its molecule, which is accompanied by elemination of water molecules.

It is essential that the second process is imposed on the first one and begins simultaneously with the melting of compound crystals. For this reason, the heat and temperature of the endothermic effects decrease upon repeated heating. The observed mass loss on the TGA curve is close to the calculated quantity of water required for self-condensation of tetraol **1**. The result of thermal polycondensation is the formation of an insoluble and sufficiently thermostable polymer product whose destructive processes occur above 400 °C. Note that the thermal behavior of compound **1** differs from that of *cis*-$[PhSi(O)OH]_4$ whose condensation (water elimination) starts at significantly lower temperatures of ~150 °C. Melting point of *cis*-$[PhSi(O)OH]_4$ lies

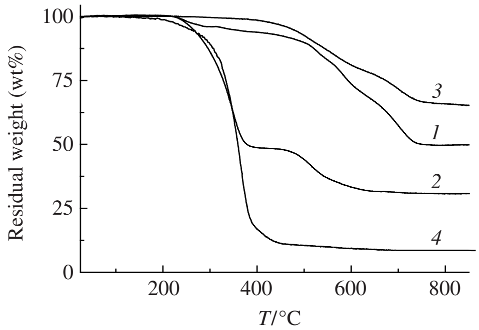

Figure 4 TGA curves for compounds (*1*), (*2*) **3a** and (*3*), (*4*) **3b** in (*1*), (*3*) air and (*2*), (*4*) argon at a heating rate 10 K min^{-1}.

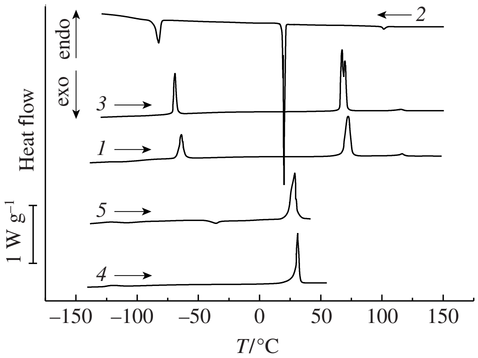

Figure 5 DSC traces for compounds (*1*)–(*3*) **3a** and (*4*), (*5*) **3b** upon (*1*), (*4*) first and (*3*), (*5*) second heating, and (*2*) cooling; the heating and cooling rates are 10 K min^{-1}.

above the polycondensation temperature and it exhibits only one broad endothermic peak on the DSC curve in the temperature range at which sample weight loss is observed.

According to the TGA data, the thermal behaviors of compound **3a** in air and in argon are substantially different (Figure 4, curves *1* and *2*). Compound **3a** loses in air at 250 °C about 5 wt% and the basic processes of thermal oxidative destruction occur near 550 °C. In argon, the loss of mass at 250 °C is substantially higher (~60 wt%). The thermal behavior of compound **3b** from TGA data (see Figure 4 curves *3*, *4*) is very similar to that of compound **3a**. It can be supposed that air oxygen initiates intermolecular reactions proceeding with participation of vinyl (compound **3a**) or hydride (compound **3b**) groups thus affording temperature-resistant material with a cross-linked structure.

The DSC curves for compound **3a** show three reversible endothermic transitions (Figure 5). The first one, occurring at $T = -64$ °C ($\Delta H = 11$ J g^{-1}), corresponds to a crystal–crystal transition; the second one, at $T = 72$ °C ($\Delta H = 24$ J g^{-1}), corresponds to melting of the crystalline phase; the third transition is very weak ($T = 116$ °C, $\Delta H = 1.5$ J g^{-1}), which is characteristic of mesophase–isotropic melt transition.

Upon the first heating, the DSC trace of compound **3b** (see Figure 5, curve *4*) reveals a jump of heat capacity at the devitrification temperature of –125 °C, a poorly defined exothermic peak corresponding to cool crystallization ($T = -110$ °C, $\Delta H = 3.9$ J g^{-1}), and an endothermic peak associated with melting of the crystalline phase ($T = 31$ °C, $\Delta H = 21$ J g^{-1}). Upon repeated heating (see Figure 5, curve *5*) at the temperature higher than a temperature of jump of heat capacity at devitrification, the wide peak of cold crystallization begins in the area of –100 °C with a minimum at $T = -35$ °C ($\Delta H = 11$ J g^{-1}), which corresponds to crystallization of the part of compound **3b** that is not converted into a crystal upon cooling under conditions of experiment, and endothermic melting peak at $T = 29$ °C ($\Delta H = 21$ J g^{-1}).

In summary, we have obtained all-*cis*-tetra(*p*-tolyl) cyclotetrasiloxanetetraol **1** and performed its functionalization affording stereoregular all-*cis*-cyclotetrasiloxanes **3a**,**b**, which can be used as starting materials for the further synthesis of star-shaped polymers. Investigations using differential scanning calorimetry and polarized optical microscopy revealed mesomorphic properties of compound **3a**. A full account on these properties will be published elsewhere. In continuation of our studies on star-shaped polysiloxanes,[24] the new compounds will be used for the preparation of new type of amphiphilic star-shaped siloxanes.

This work was supported by the Russian Science Foundation (grant no. 14-23-00231). The NMR, IR spectroscopic and X-ray data were obtained using the equipment of Center for Molecule Composition Studies of A. N. Nesmeyanov Institute of Organoelement Compounds, Russian Academy of Sciences.

Online Supplementary Materials

Supplementary data associated with this article can be found in the online version at doi: 10.1016/j.mencom.2018.07.026.

References

1 R. H. Baney, M. Itoh, A. Sakakibara and T. Suzuki, *Chem. Rev.*, 1995, **95**, 1409.

2 R. H. Baney and X. Cao, in *Silicon-Containing Polymers: the Science and Technology of Their Synthesis and Applications*, eds. R. G. Jones, W. Ando and J. Chojnowski, Kluwer Academic Publishers, Dordrecht, 2000, ch. 6, pp. 157–184.

3 M. Unno, A. Suto and T. Matsumoto, *Russ. Chem. Rev.*, 2013, **82**, 289.

4 Z. Chen, Z. Li, H. Guo, J. Zhang, Z. Ren, S. Yan, P. Xie and R. Zhang, *Chem. Mater.*, 2012, **24**, 1968.

5 A. S. S. Lee, S.-S. Choi, H. S. Lee, H. Y. Jeon, K.-Y. Baek and S. S. Hwang, *J. Polym. Sci., Part A*, 2012, **50**, 4563.

6 S. Chang, T. Matsumoto, H. Matsumoto and M. Unno, *Appl. Organomet. Chem.*, 2010, **24**, 241.

7 S. Watase, D. Fujisaki, M. Watanabe, K. Mitamura, N. Nishioka and K. Matsukawa, *Chem. Eur. J.*, 2014, **20**, 12773.

8 H. S. Lee, S.-S. Choi, K.-Y. Baek, E. C. Lee, S. M. Hong, J.-C. Lee and S. S. Hwang, *Macromol. Res.*, 2012, **20**, 1131.

9 X. Wang, J. Li and L. Wu, *Polym. Adv. Technol.*, 2011, **22**, 2151.

10 M. Unno, Y. Kawaguchi, Y. Kishimoto and H. Matsumoto, *J. Am. Chem. Soc.*, 2005, **127**, 2256.

11 F. J. Feher, J. J. Schwab, D. Soulivong and J. W. Ziller, *Main Group Chem.*, 1997, **2**, 123.

12 M. Unno, K. Takada and H. Matsumoto, *Chem. Lett.*, 1998, **27**, 489.

13 M. Unno, Y. Kishimoto and H. Matsumoto, *Organometallics*, 2004, **23**, 6221.

14 V. Lorenz, K. Jacob, C. Wagner and H. Z. Goerls, *Z. Anorg. Allg. Chem.*, 2002, **628**, 2855.

15 O. I. Shchegolikhina, Yu. A. Pozdnyakova, Yu. A. Molodtsova, S. D. Korkin, S. S. Bukalov, L. A. Leites, K. A. Lyssenko, A. S. Peregudov, N. Auner and D. E. Katsoulis, *Inorg. Chem.*, 2002, **41**, 6892.

16 P. Jutzi, G. Strassburger, M. Schneider, H.-G. Stammler and B. Neumann, *Organometallics*, 1996, **15**, 2842.

17 Yu. A. Pozdnyakova, A. A. Korlyukov, E. G. Kononova, K. A. Lyssenko, A. S. Peregudov and O. I. Shchegolikhina, *Inorg. Chem.*, 2010, **49**, 572.

18 A. Kowalewska and M. Nowacka, *Silicon*, 2015, **7**, 133.

19 Yu. N. Kononevich, A. A. Anisimov, A. A. Korlyukov, U. S. Tsareva, O. I. Shchegolikhina and A. M. Muzafarov, *Mendeleev Commun.*, 2017, **27**, 332.

20 A. A. Anisimov, P. V. Zhemchugov, S. A. Milenin, A. S. Goloveshkin, U. S. Tsareva, I. S. Bushmarinov, A. A. Korlyukov, R. U. Takazova, Yu. A. Molodtsova, A. M. Muzafarov and O. I. Shchegolikhina, *J. Organomet. Chem.*, 2016, **823**, 103.

21 F. Yagihashi, M. Igarashi, Y. Nakajima, K. Sato, Y. Yumoto, C. Matsui and S. Shimada, *Eur. J. Inorg. Chem.*, 2016, 2882.

22 R. Ito, Y. Kakihana and Y. Kawakami, *Chem. Lett.*, 2009, **38**, 364.

23 M. Unno, K. Takada and H. Matsumoto, *Chem. Lett.*, 2000, **29**, 242.

24 Yu. S. Vysochinskaya, V. V. Gorodov, A. A. Anisimov, K. L. Boldyrev, M. I. Buzin, A. V. Naumkin, K. I. Maslakov, A. S. Peregudov, O. I. Shchegolikhina and A. M. Muzafarov, *Russ. Chem. Bull., Int. Ed.*, 2017, **66**, 1094 (*Izv. Akad. Nauk, Ser. Khim.*, 2017, 1094).

Received: 8th December 2017; Com. 17/5427